Cyclic Oxidation Behavior of CoNiCrAlY Coatings Produced by LVPS and HVOF Processes†

MOHAMMADI Majid*, JAVADPOURA Sirus*, KOBAYASHI Akira, SHIRVANI Korush***, JENABALI JAHROMI Ahmad*, KHAKPOUR Iman***

Abstract

CoNiCrAlY bond coatings for thermal barrier systems were produced by low vacuum plasma spray (LVPS) and high velocity oxy fuel (HVOF) on the nickel base superalloy, IN738LC. High temperature cyclic oxidation resistance of coated samples was performed in 1100℃ for 100 cycles including 1h holding at high temperature and cooling to room temperature by air flow. Oxidation kinetics were determined by weight gain measurement of samples in each cycle, microstructural characterizations of coatings and oxide scales were investigated by scanning electron microscope equipped with EDS, and X-ray diffraction methods. The results proved better cyclic oxidation of CoNiCrAlY-HVOF coatings at the initial stage of oxidation and better oxidation behavior of LVPS coatings at continuation. The enhanced cyclic oxidation resistance of the HVOF coating at the initial stage was due to the nucleation of α-Al_2O_3 during the coating process and formation of continuous protective oxide layer at the initial stage of oxidation, but at continuation, large grain oxide, unsuitable adherence and existence of some microcracks in the TGO cause to easily spallation and severe oxidation in the HVOF samples was observed.

KEY WORDS: (CoNiCrAlY coating), (HVOF), (LVPS), (Cyclic oxidation), (TGO), (Spallation)

1. Introduction

Materials for producing energy in the turbine engine, must be able to operate in the high temperature gases (above 1400ºC) emerging from the combustion chamber. They experience a combination of high temperatures, mechanical and thermal stresses [1-3]. Accordingly, the development of nickel-based superalloys has, almost entirely, been motivated by the requirement to improve the efficiency, reliability and operating life of gas turbines since the 1940s [1-3]. Protection of these alloys against hot corrosion and oxidation is typically conferred by the application of either diffusion or overlay metallic coating that is able to form a continuous, adherent, and slow-growing oxide scale. The most widely used diffusion coatings are based on the aluminide β-NiAl, while overlay coatings are typically based on a MCrAlY composition in which M represents Ni, Co, or Ni + Co [1-10].

Extensive research efforts over decades led to advanced protective coatings for turbine components, primarily for thermal insulation as well as to enhance the oxidation/hot corrosion resistance of turbine components [1,2]. Therefore the duplex protective systems that consist of overlay MCrAlY bond coat (BC) and ceramic top coat (TC) such as 8wt.% yttria partially stabilized zirconia (8PYSZ) are used mainly in the turbine component and aero engines against high temperature oxidation and corrosion. This protective system, called thermal barrier coating (TBC), allows the increase of the gas inlet temperature without raising the base metal temperature [1-10].

The service-life of MCrAlY coatings depends greatly on the aluminum and chromium content, depletion of aluminum and chromium in order to form and re-heal the protective oxide layer is the main reason of degradation in these coatings [9,10]. Formation of adherent, continuous, dense, and stable protective oxides, is affected by factors such as chemical composition of MCrAlY coating, environmental condition, working temperature and coating processes [1,2,10].

Effect of different coating processes on the oxidation and hot corrosion resistance of these coatings were examined by many researchers, Diana and et al, determined the oxidation behavior of VPS and HVOF MCrAlY coatings, and found that formation of the metastable alumina in the VPS coating leads to a fast oxidation rate. In the HVOF-sprayed coatings, only continuous and stable α-Al_2O_3 with low growth rate was

† Received on June 10, 2011
* Shiraz University
** Associate Professor
*** Associate Professor

Transactions of JWRI is published by Joining and Welding Research Institute, Osaka University, Ibaraki, Osaka 567-0047, Japan

created after a short oxidation time [11]. It seems that the fine oxide dispersion formed in HVOF-sprayed MCrAlY coatings has a beneficial effect on the high-temperature oxidation behavior of the coatings [11]. According to the Brandl and et al, investigations, the oxidation kinetics of the VPS and HVOF sprayed MCrAlY coatings are very different and oxidation rate of the HVOF sprayed coating is considerably lower than that of the VPS coatings [12].

In the present study, cyclic oxidation properties and oxide behavior of the CoNiCrAlY coatings, prepared by two-difference process: (1) low vacuum plasma spray (LVPS) and (2) high velocity oxy fuel (HVOF) on the IN738LC, were investigated and compared.

2. Experimental

2.1. Sample preparation

The substrate alloys used in this study were Ni-base superalloys IN738LC, which have been used in the turbine engine blades. CoNiCrAlY coatings were deposited using high velocity oxy-fuel (HVOF) and low vacuum plasma spray (LVPS) technique. **Table 1** shows the nominal composition of the IN738LC alloy and the CoNiCrAlY coating that were used in this study. Prior to the bond coat deposition, rectangular samples with the dimensions of 15×10×2 mm were ground using No. 1000 SiC abrasive paper and were grit-blasted with alumina powder in order to increase adherence between the coating and the substrate and then ultrasonically cleaned in ethanol. An HVOF spray system (Metallisation MET-JET II) with a spraying distance of 38 cm and spray fuel of kerosene (C_7H_{16}). Oxygen flow rate, fuel flow rate and powder feed rate were regulated as follows: 900 l/min, 200 ml/min, and 55 g/min have been used for bond coat deposition of both sides of samples. Coating thickness was about 300 μm. Samples were solution and aging heat-treated for 4 h at 1100℃ and 20 h at 850℃ in a vacuum furnace respectively.

2.2. Cyclic oxidation test

Cyclic oxidation resistance of the coated samples was measured in an air environment at 1100℃ for 100 cycles in a thermal cycling furnace. Each cycle consists of 1 h heating at 1100℃ followed by 20 min cooling to room temperature by air force cooling [7,13]. The weight change of specimens was measured at the end of each cycle with an accurate electronic balance in order to determine the oxidation kinetics. Some samples are selected at diverse cycles in order to characterize and investigate oxide scale and coating microstructure with SEM, EDAX, and XRD analysis.

3. Results

3.1. As-Coated samples

Fig. 1 shows the SEM images of the heat treated LVPS and HVOF CoNiCrAlY coatings. This shows, a dual-phase structure consisting of an fcc structure austenitic solid solution γ, a bcc intermetallic phase, β-NiAl and γ′-Ni_3Al intermetallic compound presented as light and dark areas respectively [1,5,8,11]. Further, some oxide particles can be detected on the some parts of the HVOF coating. The application of HVOF-spraying induces partial oxidation of metallic powder particles [5].

X-ray diffraction patterns for as-sprayed LVPS and HVOF coatings after heat treating are shown in **Fig. 2**, the coatings are mainly consist of γ solid solution, γ′-Ni_3Al and β-(Co,Ni)Al phase and a minor of α-Al_2O_3 peak that is more stronger in HVOF samples, this phase can be produced during coating and heat treatment processes[11].

Table 1 Nominal composition of IN-738LC and CoNiCrAlY coating that used in this research.

Material	Chemical Composition
IN738LC	61.7%Ni-15.5%Cr-8.5%Co-3.5%Al-3.5%Ti-2,6%W -1.8%Mo-1.6%Ta-Trace
CoNiCrAlY Powder	Co-29%Ni-26%Cr-8%Al-0.6Si-0.8%Y

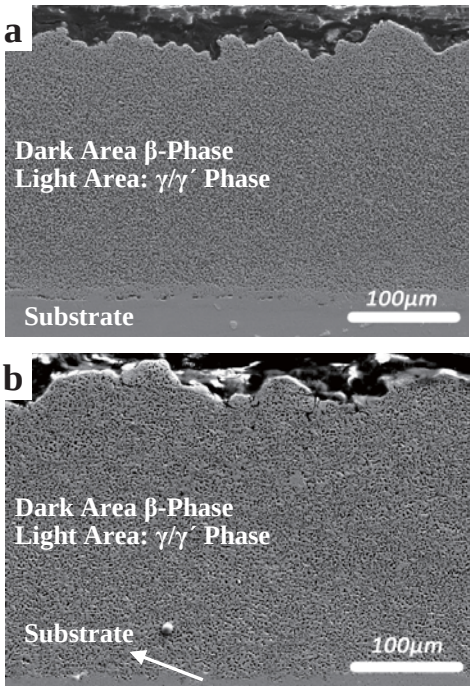

Fig. 1 Cross-section microstructure of as-coated samples after vacuum heat treatment. a- LVPS b- HVOF coating

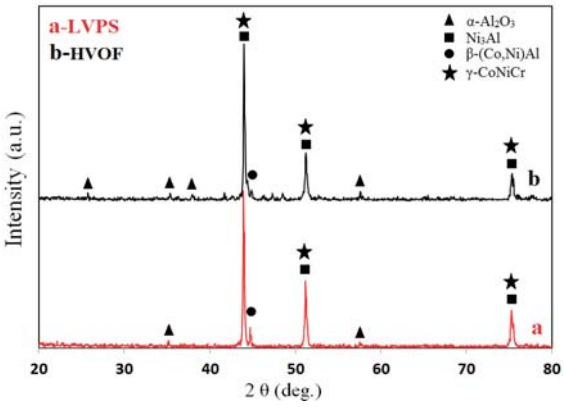

Fig 2. X-ray diffraction patterns for as-sprayed CoNiCrAlY coatings after heat treating.

3.2. Oxidation test

Fig. 3 shows the oxidation kinetic and spallation curves of LVPS and HVOF specimens exposed in air at 1100 ◦C for 100 h. The mass changes shown in this diagram consist of a mass gain owning to the oxidation and a mass loss due to the spallation of oxide scales during cooling and heating [14,15]. The maximum weight gains of specimens were ‐ 2.65mg/cm^2 and ‐ .7mg/cm^2 for LVPS and HVOF coatings respectively.

The LVPS coating shows a rapid mass gain from the beginning of cyclic oxidation and after an initial transient period, the steady state oxidation kinetics of the LVPS decreased to near-parabolic rates, indicating a continuous and protective oxide scale forming on the bond coat [7]. No visible spallation damage of the LVPS was found during the test. In HVOF coating, oxidation happens more gradually with slower rate at the beginning, but oxide spallation overcome to the oxidation just after ~ 15 cycles, although a steady state condition appear after that, but some oscillation in the kinetic curve proving that easily spallation of protective oxide happens during the cyclic oxidation test [15]. Finally the HVOF coated samples fail after 78 cycles due to severe oxidation and easily spallation of TGO [15]. For LVPS samples oxidation can be reported as a dominant mechanism in all of the test periods and after 100 cycles of oxidation these coatings resist against severe oxidation.

Cross sectional microstructure of LVPS and HVOF-CoNiCrAlY coatings after 10 cycles of oxidation in laboratory condition and 1100 ℃ are shown in **Fig. 4**. In addition to the β-NiAl and γ phases, it displays an oxide scale and clearly a β-NiAl depleted zone in the boundary of coating and oxide layer formed on the coating. It is well known that CoNiCrAlY coatings protect the substrate superalloy against oxidation and hot corrosion by forming a protective oxide layer. Therefore, any replacement in oxide scale feature may change the degradation rate [7,10,15]. Fig. 4 shows two different oxide scales for HVOF and LVPS where they are exposed to cyclic oxidation conditions.

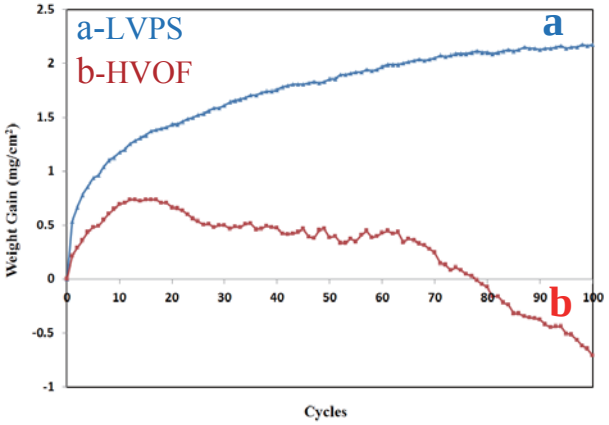

Fig. 3 Mass change as a function of number of cyclic oxidation exposures 1100 ℃ for 100 h.

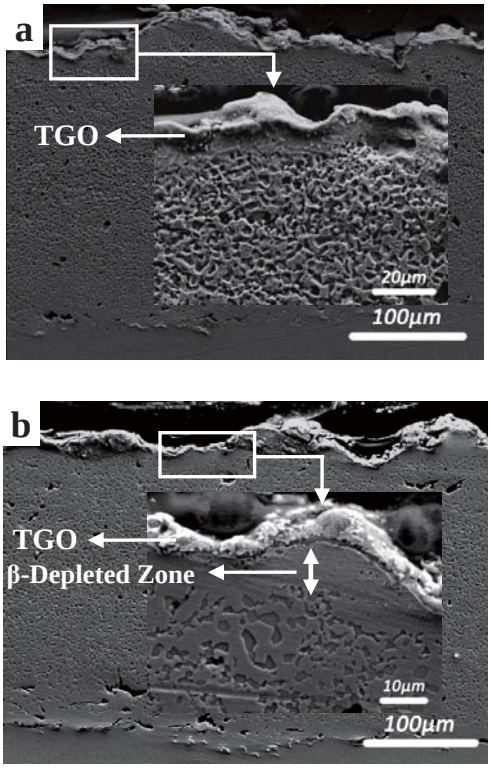

Fig. 4 Backscatter electron microstructure of coating after 10h cyclic oxidation at 1100 °C for a- LVPS and b- HVOF-CoNiCrAlY coatings.

Fig. 5 shows the XRD patterns of the oxide scale produced on the LVPS and HVOF coatings after 10-cycles of oxidation. Oxide scale in HVOF samples was mainly composed of NiO, α-Al_2O_3, Co_3O_4.The existence of β peaks in this sample show that protective oxide scale is very thin and non-continuous oxide scale produced on the top of the surface. For the LVPS coatings, protective oxide scale was composed mainly of, α-Al_2O_3 and no β phase has been observed. This mean

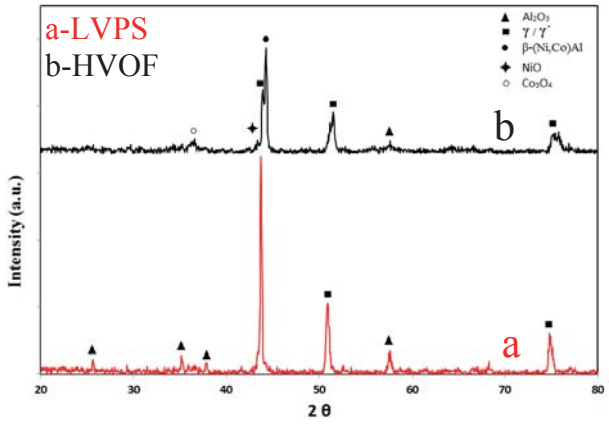

Fig. 5 XRD patterns of the CoNiCrAlY coating (a) LVPS- and (b) HVOF samples after 10 cycles of oxidation at 1100℃.

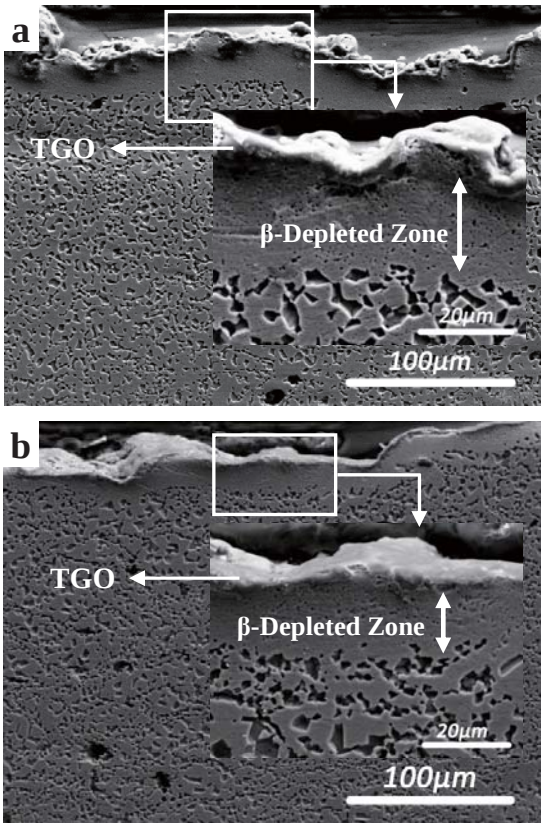

Fig. 6 Backscatter electron microstructure of coating after 75 cycle oxidation at 1100 °C for a- LVPS and b- HVOF-CoNiCrAlY coating.

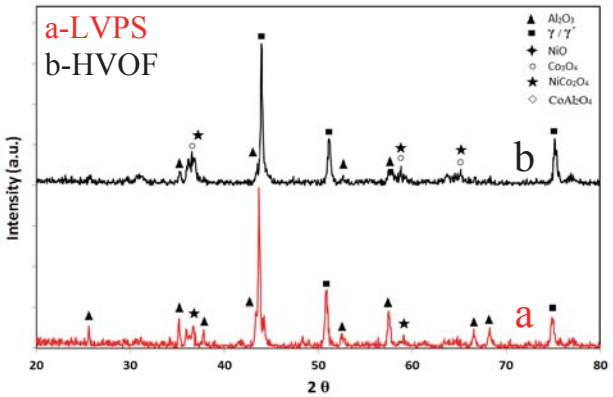

Fig. 7 XRD patterns of the CoNiCrAlY coating (a) LVPS- and (b) HVOF- samples after 75 cycles of oxidation at 1100℃.

that formation of oxide scale is more rapid than HVOF samples, this result also can be deduced from the weight gain measurement in the Fig.3.

Back scatter electron microstructure of LVPS and HVOF coatings after 70 cycles of oxidation in 1100℃ have been shown in **Fig. 6**. As it can be seen, continuous oxide scale has been formed on the both kinds of coatings and the thickness of β-depleted zones are increased but it appears that this region is wider in the LVPS coatings due to high oxidation rate in comparison to the HVOF coatings. In this situation the approximate oxide thickness of the LVPS and HVOF samples are about 5-8 μm and 5-10 μm respectively.

XRD analysis of oxide scale after 75 cycles of oxidation is given in **Fig. 7** show that the oxide scale, formed on the HVOF coating specimen is composed of mixed oxides. Moreover, the peak intensity of other unsuitable oxides such as NiO and Co_3O_4 has been increased. The thickness of β-(Ni,Co)Al depleted zone is more in the LVPS coating than HVOF coating. This can be due to the consumption of Al and growth of oxide scale [15].

Cross sectional microstructural of CoNiCrAlY bond-coats after 100-cycle of oxidation at 1100 °C have been shown in **Fig. 8**. Increase of the β-depleted zone in the LVPS coating is in good agreement to the oxidation kinetic curve. In these coatings, β-NiAl acts as an aluminum reservoir for the formation of the protective alumina oxide layer. As the protective oxide spalls during oxidation, aluminum in the coating diffuses outwards to rehabilitate the protective surface oxide layer [7,8,14,15]. Depletion of aluminum near the surface, leads to transformation of β-NiAl in to γ′-Ni_3Al and prolonging of oxidation causes growth of this area and transformation of γ′-Ni_3Al in to γ-solid solution and as a result of which, the coating degrades[10,16]. Oxidation of γ phase in the β-depleted zone occurred in both types of coatings but it

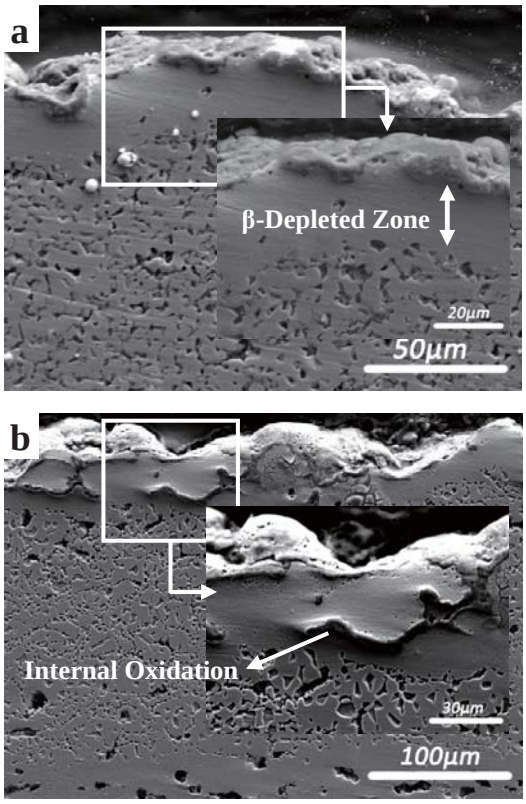

Fig. 8 Backscatter electron microstructure of coating after 100-cycles of oxidation at 1100 °C for a- LVPS and b- HVOF coating show additional growth of β-depleted zone and TGO in the LVPS samples and internal oxidation in HVOF coatings.

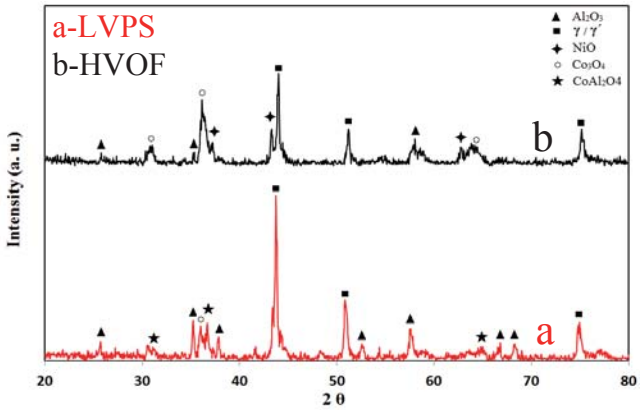

Fig. 9 XRD patterns of the (a) LVPS samples and (b) HVOF samples after 100 cyclic oxidation at 1100 ℃.

seems that this type of oxidation is more severe in the HVOF samples. Oxidation of other elements in the coatings caused, easy spallation of oxide scale during the cyclic test due to thermal stresses and low adherence of this scale [15].

According to the XRD results, in the HVOF samples replacement of another oxide such as NiO, Co_3O_4 and spinel type oxide is the main reason for spallation and some oscillation in the kinetics curve [15]. Small thicknesses of β-depleted zone and absence of internal oxides in LVPS samples after 100-cycle of oxidation in Fig. 8-b show that, these coatings have a good resistance in oxidation condition.

XRD analysis of oxide scales after 100 cycles of oxidation at 1100 ^{o}C are shown in **Fig. 9**. According to this result it can be concluded that LVPS samples have better condition and resistance to cyclic oxidation due to ability of formation and rehabilitation of alumina protective oxide. Easily spallation of HVOF coatings in contrast to the LVPS and the long time required for aluminum diffusion in to the surface, cause internal oxidation and formation of other oxide elements such as Ni and Co on the top of β-depleted zone [15,16]. In LVPS samples the main surface oxide after 100 cycles of oxidation is Al_2O_3 and some spinel compounds such as $CoAl_2O_4$ and $NiAl_2O_4$ were detected in the oxide scale, Presence of adherent and dense Al_2O_3 in the LVPS oxide scale after 100 cycles of oxidation is the main reason for good oxidation properties of LVPS samples [10,15]. The intensity of unsuitable oxides such as NiO and Co_3O_4 has been increased In the HVOF sample after 100 cycles of oxidation.

Fig. 10, shows the surface morphology of two type of coatings after 100 cycles of oxidation, It is cleared that particle sizes of oxide scale is different in the two types of coatings and some microcracks are observed between oxide particles in the HVOF samples. HVOF morphology consists of coarse and fine oxide particles and some valley and lumps can be seen over all of the surface. Porous structure of protective oxide scale and existence of intergranular cracks can affect the coating life time by two factors, first is the higher oxidation rate due to high

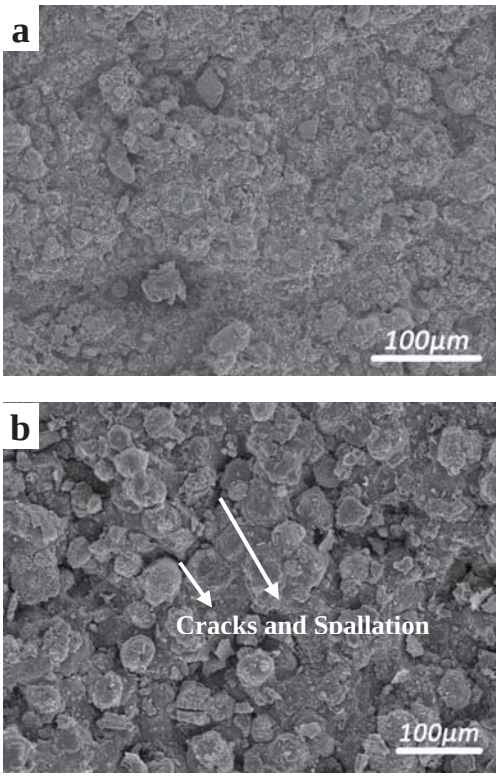

Fig. 10 surface morphology of CoNiCrAlY coating after 100 cycles of oxidation, a-LVPS and b. HVOF

oxygen diffusion path [15], this factor can lead to internal oxidation that can be seen in the Fig. 8, another factor is easy and severe spallation during thermal cycling oxidation due to thermal stresses and strains in the oxide particle interface, this factor caused some oscillation in kinetic curve [15].

In LVPS sample, continuous oxide scale covered all of the surface and no cracks and severe spallation can be detected. Initial surface condition such as surface roughness, bond coating grain size and coating condition have important effect on the oxidation properties of metallic coatings.

Formation of the fine and dispersed Al_2O_3 during the HVOF process has been reported by many investigators, according to this results α-Al_2O_3 particles that are produced during thermal spraying can act as initial nuclei and promote development of a protective TGO scale. In other coating processes such as VPS it has been reported that formation of the metastable alumina coating leads to a fast oxidation rate [4,6,12,13]. Presence of more α-Al_2O_3 particle in the HVOF sample that were shown in Fig. 2, is the main reason for less oxidation rate of this coating at the first stage of oxidation, but at continuation other factors such as oxide adherence, surface roughness, oxide morphology, oxide growth rate and rehabilitation of damaged TGO, control the oxidation behavior [12, 13,15]. According to Yuan and et al, the coarse surface roughness of the bond coat has a detrimental effect on the oxidation behavior of the TBC system due to a large specific surface area [17].

Poor oxidation properties of HVOF samples can be attributed to several parameters, first is the large particle size of oxide scale that can cause more strain in the particle interface during heating and cooling [18,19]. It is clear that small grain particles have more grain boundary area and some of the strain can be damped in the interface, so a small particle size cause less stress in the grain boundary and longer life time of the protective TGO. Further fine grains also can improve the mechanical properties and thermal shock resistance of oxide scale [20], You and et al study the effect of grain size on thermal shock resistance of Al_2O_3–TiC ceramics, the results show that, fine grains of oxide improve the, fracture toughness and thermal shock resistance, attributed to suppression of crack initiation and propagation by the mechanisms of crack blunting, micro-cracks and cracks deflection [20].

Second factor is the surface roughness of the HVOF samples, according to Haynes et al, Cr_2O_3 and spinels were observed besides α-Al_2O_3 on an as-sprayed NiCoCrAlY LPPS coating surface using high temperature XRD, whereas on the polished surface of the same coating a coherent α-Al_2O_3 scale with inclusion of $YAlO_3$ was observed, further high roughness surface increased the surface area of the coating exposed to oxidation [3,17]. The final factor that affected the cyclic oxidation life of the HVOF coatings is the existence of some microcracks between the oxide particles, these cracks that are produced due to thermal stresses can act as a rapid diffusion path for oxygen and increase the oxidation rate [15].

4. Conclusion

The microstructure of oxide scales formed on HVOF and LVPS-CoNiCrAlY coatings on the IN738LC superalloy during thermal shock cycling were studied in this research. From the present results, the following conclusions can be drawn

(1) Formation of non-protective oxides such as NiO, Co3O4 on the top of HVOF- CoNiCrAlY coating, formation of coarse oxide particle and assistance of microcracks cause easily spallation and degradation of this coating in cyclic oxidation.

(2) LVPS-CoNiCrAlY coatings show better oxidation properties in contrast to HVOF coatings, due to formation of adherent, stable and dense protective oxides.

(3) Fine oxide morphologies and small grain size of coatings can improve the mechanical properties and resistance to the thermal stresses of TGO.

References

1) G.W. Goward; Surface and Coatings Technology, Vol. 108–109, 1998, p73–79.
2) M.J. Pomeroy; Materials and Design, Vol. 26, 2005, p223–231.
3) N. Czecha, M. Juez-Lorenzob, V. Kolarikb, W. Stamma, Surface and Coatings Technology, Vol. 108–109, 1998, p36–42.
4) Martina Di Ferdinando and et al, Surface & Coatings Technology, Vol. 204, 2010, p2499–2503.
5) Lidong Zhao, Maria Parco, Erich Lugscheider, Surface and Coatings Technology, Vol. 179, 2004, p272–278.
6) Leonardo Ajdelsztajn and et al, Materials Science and Engineering , Vol. A338, 2002, p33-43.
7) B. Wang and et al, Surface and Coatings Technology, Vol. 149, 2002, p70–75.
8) I. Gurrappa, A. Sambasiva Rao, Surface & Coatings Technology, Vol. 201, 2006, p3016–3029.
9) Alessio Fossati and et al, Surface & Coatings Technology, Vol. 204, 2010, p3723–3728.
10) S.M. Jiang, H.Q. Li, J. Ma, C.Z. Xu, J. Gong, C. Sun, Corrosion Science, Vol. 52, 2010, p2316–2322.
11) Diana Toma, Waltraut Brandl, Uwe Ko ster, Surface and Coatings Technology, Vol. 120–121, 1999, p8–15.
12) W. Brandl, D. Tomaa , H.J. Grabke, Surface and Coatings Technology, Vol.108–109, 1998, p10–15.
13) A. Nusair Khan, J. Lu, Surface & Coatings Technology, Vol. 201, 2007, p4653–4658.
14) W.R. Chen and et al, Surface & Coatings Technology, Vol. 202, 2008, p2677–2683.
15) J. R. Nicholls and M. J. Bennett; Material at High Temperature, Vol. 17(3), 2000, p. 413-428.
16) R. Mobarra, A.H. Jafari, M. Karaminezhaad, Surface & Coatings Technology, Vol. 201, 2006, p2202–2207.
17) F.H. Yuan and et al, Corrosion Science, Vol.50, 2008, p1608–1617.
18) Q.M. Wang and et al; Materials Science and Engineering, Vol. A 406, 2005, p337–349.
19) Q.M. Wang and et al; Materials Science and Engineering, Vol. A 406, 2005, p350–357.
20) Sylvain Fayette and et al, Journal of the European Ceramic Society, Vol. 20, 2000, p297-302.